NASA/TM—2018–220124

Iodine Propellant Feed System Flow Modeling

A.K. Martin, P. Sawicki, and K.A. Polzin
Marshall Space Flight Center, Huntsville, Alabama

October 2018

The NASA STI Program…in Profile

Since its founding, NASA has been dedicated to the advancement of aeronautics and space science. The NASA Scientific and Technical Information (STI) Program Office plays a key part in helping NASA maintain this important role.

The NASA STI Program Office is operated by Langley Research Center, the lead center for NASA's scientific and technical information. The NASA STI Program Office provides access to the NASA STI Database, the largest collection of aeronautical and space science STI in the world. The Program Office is also NASA's institutional mechanism for disseminating the results of its research and development activities. These results are published by NASA in the NASA STI Report Series, which includes the following report types:

- TECHNICAL PUBLICATION. Reports of completed research or a major significant phase of research that present the results of NASA programs and include extensive data or theoretical analysis. Includes compilations of significant scientific and technical data and information deemed to be of continuing reference value. NASA's counterpart of peer-reviewed formal professional papers but has less stringent limitations on manuscript length and extent of graphic presentations.

- TECHNICAL MEMORANDUM. Scientific and technical findings that are preliminary or of specialized interest, e.g., quick release reports, working papers, and bibliographies that contain minimal annotation. Does not contain extensive analysis.

- CONTRACTOR REPORT. Scientific and technical findings by NASA-sponsored contractors and grantees.

- CONFERENCE PUBLICATION. Collected papers from scientific and technical conferences, symposia, seminars, or other meetings sponsored or cosponsored by NASA.

- SPECIAL PUBLICATION. Scientific, technical, or historical information from NASA programs, projects, and mission, often concerned with subjects having substantial public interest.

- TECHNICAL TRANSLATION. English-language translations of foreign scientific and technical material pertinent to NASA's mission.

Specialized services that complement the STI Program Office's diverse offerings include creating custom thesauri, building customized databases, organizing and publishing research results…even providing videos.

For more information about the NASA STI Program Office, see the following:

- Access the NASA STI program home page at <http://www.sti.nasa.gov>

- E-mail your question via the Internet to <help@sti.nasa.gov>

- Phone the NASA STI Help Desk at 757–864–9658

- Write to:
  NASA STI Information Desk
  Mail Stop 148
  NASA Langley Research Center
  Hampton, VA 23681–2199, USA

NASA/TM—2018–220124

Iodine Propellant Feed System Flow Modeling

A.K. Martin, P. Sawicki, and K.A. Polzin
Marshall Space Flight Center, Huntsville, Alabama

National Aeronautics and
Space Administration

Marshall Space Flight Center • Huntsville, Alabama 35812

October 2018

Acknowledgments

The authors wish to express their thanks to Anita Beatty for her aid in assembling this document. The authors acknowledge and thank Christine Greve, Stephen Samples, and Alex Trujillo for their contributions to this work. The authors also thank Alok Majumdar and Andre Leclair for their helpful advice and suggestions on implementing a low pressure, low flow rate iodine vapor model into the Generalized Fluid System Simulation Program. This work was sponsored by NASA's Space Technology Mission Directorate and was managed by the Small Spacecraft Technology Program at the NASA Ames Research Center.

TRADEMARKS

Available from:

NASA STI Information Desk
Mail Stop 148
NASA Langley Research Center
Hampton, VA 23681–2199, USA
757–864–9658

This report is also available in electronic form at
<http://www.sti.nasa.gov>

TABLE OF CONTENTS

LIST OF FIGURES

LIST OF FIGURES (Continued)

LIST OF ACRONYMS AND SYMBOLS

BaO	barium oxide
CFD	computational fluid dynamics
GFSSP	Generalized Fluid System Simulation Program
GRC	Glenn Research Center
HET	Hall-effect thruster
HOV	hand-operated valve
I_2	molecular iodine
iSAT	iodine satellite
LFE	laminar flow element
LV	latch valve
MKSI	MKS Instruments
MSFC	Marshall Space Flight Center
N_2	molecular nitrogen
NIST	National Institute of Standards and Technology
JANAF	Joint Army Navy Air Force
PFCV	proportional flow control valve
PFS	propellant feed system
SI	international system of units
SOV	solenoid operated valve
SS	stainless steel

NOMENCLATURE

A	exposed surface area
a	constant
C_f	flow coefficient
C_P	specific heat at constant pressure
C_V	specific heat at constant volume
H	enthalpy
I_{sp}	specific impulse
k	Boltzmann's constant
M	molar mass
m	mass
m_{amu}	mass of one amu
m_m	molecular mass
M_{I2}	molecular mass of I_2
n	number density
P	ambient pressure
P_{down}	pressure downstream
P_{meas}	measured pressure
P_{up}	pressure upstream
P_{vap}	vapor pressure
R	universal gas constant

NOMENCLATURE (Continued)

r_{VdW}	Van der Waal's radius
S	entropy
S_0	entropy at given temperature
S_{meas}	measured entropy
T	temperature
T_{meas}	measured temperature
T_0	fitting parameter
t	time
U	internal energy (in joules)
V	volume
v	velocity
α	sticking coefficient
Γ	mass flow rate
γ	ratio of specific heats
Δm	change in mass
Δv	change in velocity
κ	thermal conductivity
λ	mean free path
μ	viscosity
μ_{meas}	viscosity, measured
μ_0	viscosity fitting parameter

NOMENCLATURE (Continued)

ρ	mass density
σ	collision cross section
χ_r^2	goodness-of-fit parameter

Subscripts

LV	latch valve

TECHNICAL MEMORANDUM

IODINE PROPELLANT FEED SYSTEM FLOW MODELING

1. INTRODUCTION

The use of solid iodine as a propellant in Hall-effect thrusters (HETs) is currently being investigated for small-satellite applications[1]. CubeSats offer an inexpensive mode of access to space; however, they currently lack significant propulsion capability. A high specific impulse (I_{sp}) propulsion system would permit a significant change in velocity Δv to be imparted for orbital maintenance, transfers, or de-orbit maneuvers.

An electric propulsion system that uses iodine as a propellant has a number of advantages. It has an exceptionally high $\rho \times I_{sp}$ figure of merit (density multiplied by the specific impulse), meaning that it can achieve a large total Δv with a relatively low combination of propellant mass and propellant tank volume. Also, the propellant feed system operates at low pressures (a few psia at most), as opposed to the use of super-critical xenon stored at very high pressure. Low pressure operation can lower system mass while greatly reducing the risk of propellant tank rupture, making low pressure a vitally important property for propellants on secondary payloads like CubeSats, where risks must be minimized.

The iSAT mission aims to demonstrate iodine-fed HET technology, flying it in space onboard a 12U CubeSat.[2,3] In the iSAT propellant feed system (PFS), solid iodine is sublimed through heating to produce gaseous propellant that is conducted through tubing to the thruster and cathode. The sublimation process is governed by the iodine (I_2) vapor pressure, which is shown as a function of temperature in figure 1. As gaseous I_2 flows out of the tank, the gas pressure in the volume containing the solid iodine propellant is reduced until a balance between the flow of iodine out of the tank and the sublimation rate of solid iodine at the equilibrium gas pressure and chosen tank temperature is reached.

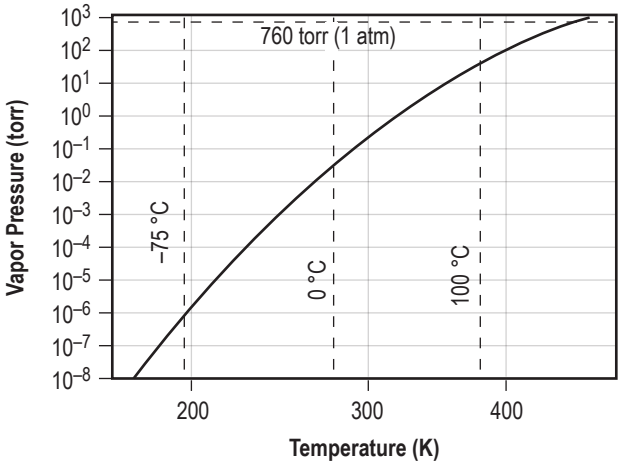

Figure 1. Vapor pressure curve for molecular iodine.[4,5]

Flow modeling was undertaken to investigate the behavior of the propellant feed system. Since iSAT is subject to both space and power limitations, the PFS will not be extensively instrumented. For example, the flight system will not have any flow-rate or pressure measurements. Control will be effected using only feedback measurements of temperature and of the electrical power drawn by the thruster anode and cathode currents. Given this limitation, it is useful to attempt to develop an understanding of how pressure and propellant flow rate correlate with the parameters that are measured. A numerical model, validated against data from more extensively instrumented laboratory tests, could fulfill this need. A flow model might also be used to explore possible operational scenarios, such as the sequencing of valves and/or heaters. It was additionally intended for this modeling to serve as a guide for the design of the iSAT PFS and potential future systems.

Much of the testing and model validation described in this report was performed using nitrogen gas (N_2). Nitrogen, like I_2, is diatomic; it is therefore assumed that the two species behave similarly in many respects and that N_2 can be used as a relatively good simulant for iodine. It is also easier to work with N_2, and there exists a wealth of data regarding its behavior over wide ranges in pressure and temperature.

2. FLOW MODELING—GENERAL CONSIDERATIONS

2.1 Generalized Fluid System Simulation Program

Numerical models of the propellant feed system and associated laboratory test configurations were implemented using the Generalized Fluid System Simulation Program (GFSSP), version 7. GFSSP is a general-purpose lumped-element computational fluid dynamics (CFD) program for modeling complex flow networks.[6] Both steady-state and unsteady fluid behavior may be modeled. In addition, one can include conjugate heat-transfer and fluid and phase mixtures. GFSSP includes extensive existing component libraries (pipes, tees, elbows, flow restrictions, etc.) with models for their flow resistance. It also contains the thermophysical properties for a variety of fluids. It includes thermal properties for a variety of solid materials, necessary when the conjugate heat transfer option is used. The code has been validated against numerous text book problems with closed form solutions and, whenever possible, against actual test data.

2.2 Iodine Properties

Fluid properties in GFSSP are supplied by the GASP/WASP and GASPAK programs, which do not include iodine. Provision for I_2 can be made in GFSSP with a user-defined fluid. This was done by selecting Fluid1 in the Edit/Options/Fluid-Options tab. Seven property files were supplied: CPFL1, HFL1, SFL1, GAMFL1, AKFL1, EMUFL1, and RHOFL1. These files contain, respectively, the specific heat at constant pressure, standard enthalpy, standard entropy, ratio of specific heats, thermal conductivity, viscosity, and density. Each of these properties is defined as a matrix over the desired pressure and temperature range.

There is not a great deal of data on the thermophysical properties of iodine, and what information is available is often given only over a limited range of conditions. For some properties, data were available over the full temperature range of interest; for other properties, values had to be extrapolated. Much of the data that were found were for I_2 at a pressure of about one atmosphere, which is much higher than the operating pressure of the propellant feed system. Data for gaseous fluorine, chlorine, and bromine were also sought, as they might serve as guides to the behavior of iodine. However, information on these other halogens was even scarcer. Where there were gaps in the iodine data, N2 was used as a guide to its behavior.

The seven fluid properties were calculated over a 51×72 matrix; 51 points uniformly spanning the pressure range from 7×10^{-5} Pa (10^{-8} psi) to 34.47 kPa (5 psi) and 72 points spanning the temperature range 10^{-8}, 100, 105, …. 450 K. The initial point in the temperature array—at essentially zero temperature ($T = 10^{-8}$ K)—was added to prevent GFSSP from going out of range during the solution iterations. The properties were converted from SI units to imperial units and written to the fluid property files for use with GFSSP. What follows is a brief description of how these fluid properties were obtained and regularized for use with GFSSP.

2.2.1 Specific Heat, Enthalpy, and Entropy

Specific heat (C_P), enthalpy (H), and entropy (S) are from the National Institute of Standards and Technology-Joint Army Navy Air Force (NIST-JANAF) tables[7], which are themselves based on a variety of sources, including experiments and *ab initio* calculations. For each of these quantities, eight discrete values over the range of 100–450 K were obtained from the reference and then interpolated to a 71-point array using the cubic-spline interpolation routine in IGOR Pro (Wavemetrics, Portland, OR). This method yields an interval of 5 K per point, which is sufficiently fine to reflect the behavior of these properties as a function of temperature. The NIST-JANAF data are given for a pressure of 1 bar; however, application of the thermodynamic relations can be used to deduce the pressure dependence of these quantities. To 0^{th} order, specific heat and enthalpy are independent of pressure. The pressure dependence of the entropy is found by considering the first law of thermodynamics:

$$TdS = dU + PdV \ , \tag{1}$$

and using the ideal-gas relation to derive the following formula[11]:

$$S(P,T) = S_0(T) - R\ln\left(\frac{P}{P_0}\right) \tag{2}$$

where

R = the universal gas constant
S_0 = the entropy (at the given temperature) at the reference pressure $P_0 = 1$ bar.

The property files were defined over 51 points in pressure up to 34.47 kPa (5 psi) in increments of 689.5 Pa (0.1 psi) with the first point at 7×10^{-5} Pa (10^{-8} psi). For comparative purposes, data for N_2 found in the NIST database[8] were taken for the same temperature and pressure range as the I_2 data. It was found for N_2 that C_P and H were indeed approximately constant as a function of pressure and that S varied with pressure according to equation (2), giving confidence in the method used to derive the properties for I_2.

2.2.2 Ratio of Specific Heats

The specific heat ratio for I_2 was calculated from the formula:

$$\gamma = C_P / C_V = C_P / (C_P - R) \ . \tag{3}$$

2.2.3 Thermal Conductivity

Data for the thermal conductivity of I_2, plotted in figure 2, were found over the range of 400–600 K.[9] For these data the pressure range cited was 26.7–59.3 kPa, although it was not stated what pressure applies for any given value of $\kappa(T)$.

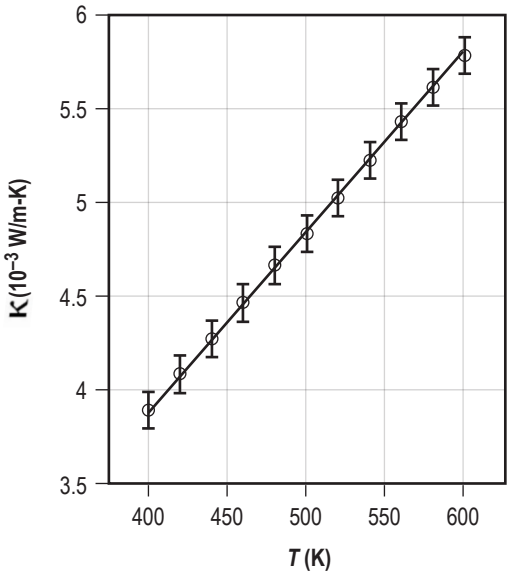

Figure 2. Thermal conductivity of I_2 as a function of temperature.[9] Also shown is a linear fit to the data, $\kappa = aT$, with $a = (9.70 \pm 0.06) \times 10^{-6}$ W/m-K^2.

The thermal conductivity of N_2 was found to vary linearly with temperature and does not vary appreciably with pressure over the entire temperature and pressure ranges of interest. By analogy, the assumptions are that the thermal conductivity of I_2 is relatively independent of pressure and that the values can be linearly extrapolated down to lower temperatures. A linear fit to these data of the form:

$$\kappa = aT \ , \tag{4}$$

resulted in a slope $a = (9.70 \pm 0.06) \times 10^{-6}$ W/m–K^2, with reduced goodness-of-fit parameter $\chi_r^2 = 0.027$.

2.2.4 Viscosity

Measurements of the viscosity of I_2, plotted in figure 3, have been reported over a temperature range of roughly 400–520 K.[10] These measurements were performed at a pressure of 6 kPa (the vapor pressure of sublimed iodine at a temperature of 373.15 K). This pressure is within the

expected operating range of the iSAT propellant feed system. As for previous properties, nitrogen was used as a guide to determining the behavior of iodine as a function of temperature and pressure. The viscosity of N_2 increases monotonically with temperature and is independent of pressure. Over the temperature range considered, μ appears to vary linearly with temperature; however, the dependence of viscosity on temperature (for temperatures > 100 K) is generally thought to be better described by Sutherland's formula:[11]

$$\mu(T) = \mu_0 \frac{(T/T_0)^{3/2}}{(1+(T/T_0))} \quad . \tag{5}$$

The data shown in figure 3 were fit with equation (5), with μ_0 and T_0 treated as fitting parameters, yielding $\mu_0 = (3.85 \pm 0.36) \times 10^{-5}$ kg/m-s, and $T_0 = (417 \pm 41)$ K, with $\chi_r^2 = 2.7$. A linear fit yielded a lower reduced fitting parameter, however it diverged significantly from the fit to equation (5) at lower temperatures. Given that Sutherland's formula is the generally accepted form for the temperature dependence of viscosity, it was used to generate the I_2 property tables over the range of interest.

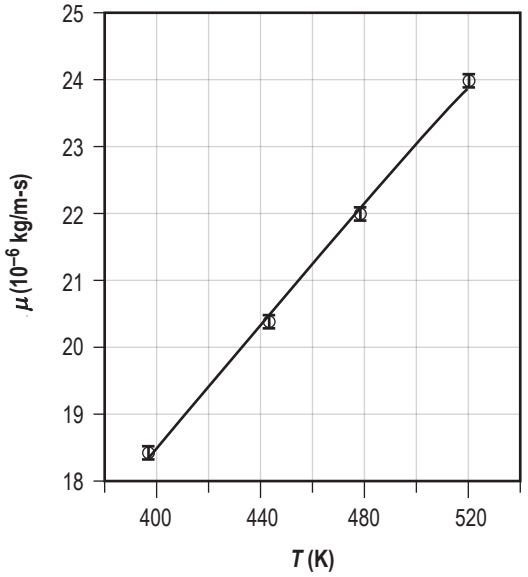

Figure 3. Measured viscosity of I_2 as a function of temperature, taken from reference 10. Also shown is a fit to the data using Sutherland's formula (eq. (5)) with $\mu_0 = (3.85 \pm 0.36) \times 10^{-5}$ kg/m-s, and $T_0 = (417 \pm 41)$ K.

2.2.5 Density

Density:

$$\rho(P,T) = m_{I2} n = \left(\frac{M_{I2} m_{amu}}{k} \right) \left(\frac{P}{T} \right) \ , \tag{6}$$

is calculated from the ideal gas law:

$$P = nkT \ , \tag{7}$$

where

k = Boltzmann's constant
M_{I2} = molecular mass of I_2 (253.809 amu)
m_{amu} = mass of 1 amu (1.660543×10^{-27} kg).

2.3 Iodine Sublimation Model

The sublimation of solid iodine into vapor was included in the GFSSP model. The quasi-steady sublimation of a solid can be calculated with an equation first proposed by Langmuir[12,13] in which the rate of mass evolution is given by:

$$\frac{dm}{dt} = \alpha A \sqrt{\frac{M}{2\pi RT}} \left(P_{vap} - P \right) \ , \tag{8}$$

where

α = sticking coefficient (usually assumed to be 1)
A = exposed surface area
M = molar mass of the solid material
R = universal gas constant
P = ambient pressure of the overlying gas
T = temperature of the overlying gas
P_{vap} = vapor pressure at the temperature of the solid being sublimed.

This equation assumes that the solid and the overlying gas are in approximate equilibrium.

The sublimation of mass into the tank was implemented in the model by including a mass source term that is governed by equation (8) in the GFSSP user subroutine BNDUSER. The rate of mass evolution in the tank node is calculated at every time-step using the updated fluid and solid node variables. A back-relaxation scheme was used to make the calculation numerically stable.

2.4 Component Models

A wide variety of components can be modeled in GFSSP and are available as standard options. Valves, for example, can be modeled with either the flow-restriction or compressible orifice option by providing a history file with a time-dependent orifice area. This approach assumes that the flow coefficient, C_f , providing the relationship between the pressure drop across the component and the corresponding flow rate is well known. This is the case for standard flow system elements, such as straight sections of tubing, elbows, and tees—and for commercially available valves—characterized for and used within their nominal operating regime.

The iSAT PFS makes use of two custom proportional flow control valves (PFCV), fabricated by VACCO Industries, Inc. (South El Monte, CA). These valves regulate the flow of propellant to the anode and cathode. The valves have not been characterized for the low flow rates that will be seen in the iSAT PFS. Likewise, the anode of the HET is a custom-built component, and its behavior is not known *a priori*. In the low Reynolds number regime of the PFS, the behavior of the valves will be dominated by the viscous flow in the boundary layer, and this will be highly dependent on the specific geometry of the component. Consequently, the flow coefficient for each component should be measured under likely operating conditions, and models for these components are needed for incorporation into the overall GFSSP model.

A procedure was developed for characterizing a given component and is described in what follows. The component in this case was a latch valve (LV), which has since been removed from the iSAT PFS baseline design; however, the procedure followed is illustrative and would be the same for any other component.

Tests of the LV were performed with N_2 as the working fluid under the assumption, discussed previously, that N_2 is a suitable simulant for I_2. The results of these tests are shown in figure 4. The LV was installed in a simple test line, plumbed with 6.35 mm (0.25 in) outer-diameter stainless-steel (SS) tubing, which is the same size tubing to be used in the actual PFS. Nitrogen was supplied from a K-bottle, and the test line was exhausted into a vacuum chamber. The volumetric flow rate through the valve was set using an MKS Instruments (MKSI) (Andover, MA) 1479A flow controller upstream of the valve. The pressure and temperature in the line were measured immediately upstream and downstream of the valve.

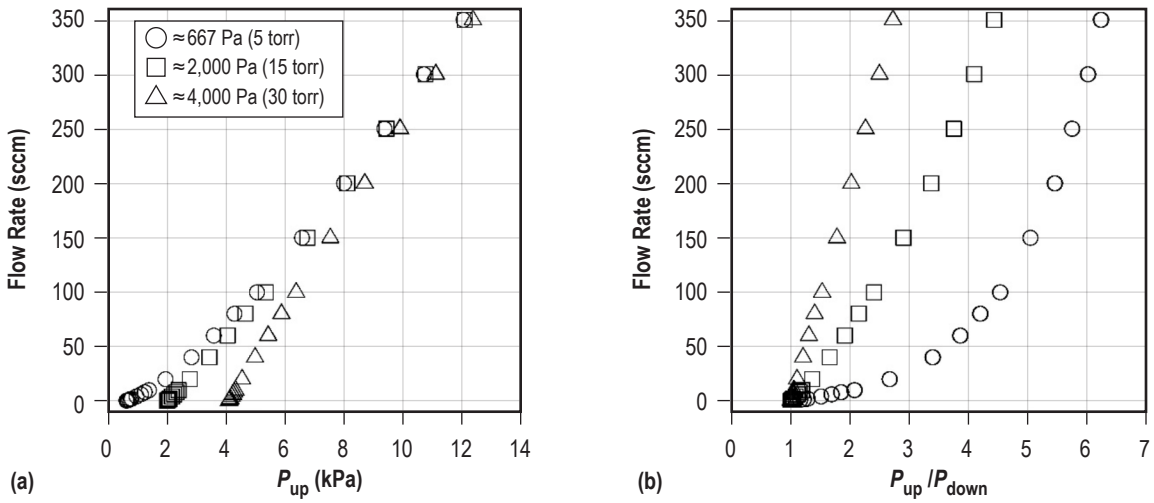

Figure 4. Volumetric N_2 flow rate through the latch valve as a function of: (a) upstream pressure and (b) the ratio of upstream-to-downstream pressure, for three values of background pressure in the exhaust chamber.

With the valve fully open and starting with a given finite background pressure in the vacuum chamber, the flow controller was stepped through increasing values of flow rate, from about 0.1 sccm to about 350 sccm; the flow was held constant at each value long enough (5–10 s) to reach an equilibrium condition. Data were obtained for chamber pressures of approximately 667 Pa, 2,000 Pa, and 4,000 Pa (5, 15, and 30 torr, respectively). Figure 4a shows the flow rate plotted versus upstream pressure, P_{up}; figure 4b shows the flow rate plotted versus the ratio of upstream to downstream pressure, P_{up} / P_{down}. These two graphs indicate the problem of parameterizing the operation of the valve in terms of the pressure. In figure 4a, although the curves all seem to approach a common limiting curve at higher values of Pup, they diverge significantly at lower pressures. In terms of P_{up} / P_{down}, the three curves are widely dispersed and no simple parameterization of the flow is apparent.

Parameterization of the flow through the device in terms of Reynolds number was suggested (A.K. Majumdar, NASA MSFC, private communication, April 2015) as being a method that could readily be integrated into a GFSSP model. The flow coefficient and Reynolds number for these data were deduced using a simple generic steady-state GFSSP model (fig. 5). The device-under-test, in this case the LV, is modeled using the compressible orifice component in GFSSP. The pressures and temperatures measured in the experiment at both the upstream and downstream test stations are specified as the boundary conditions in the external nodes of the GFSSP model. The measured volumetric flow rate was converted to a mass flow rate using tables of densities for N_2 over the relevant pressure and temperature ranges[8], and a bilinear interpolation scheme was used to determine the density for the specific measured values of upstream pressure and temperature.

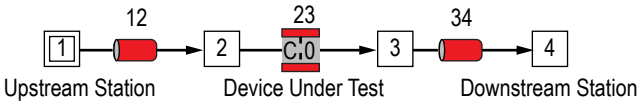

Figure 5. Generic GFSSP model for using experimental data to determine C_f for a component. Pressure and temperature are measured at both the upstream and downstream test stations.

The inputs for the compressible orifice component are the cross-sectional area and C_f. The area for the LV when open is 1.94×10^{-6} m^2 (0.003 in^2)(J. Cardin, VACCO Industries, Inc., private communication, June 2015). The flow coefficient was varied until the flow rate predicted by GFSSP equaled the measured value (the agreement in flow rate was typically good to three or four significant figures), and this value of C_f and the Reynolds number calculated by GFSSP were both recorded. The resulting curves of C_f (Re) are shown in figure 6.

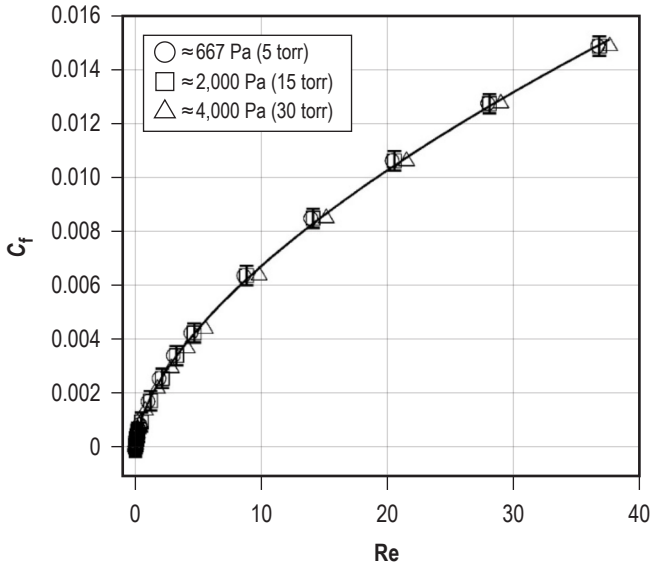

Figure 6. Flow coefficient as a function of Reynolds number for the VACCO latch valve, as deduced with GFSSP. Data for three separate trials with different back pressures. The error bar for C_f is ±0.00036.

The results from all three tests collapse to one curve with relatively little dispersion, indicating that parameterizing C_f in terms of Reynolds number is a much better approach than parameterizing it in terms of pressure or pressure ratio. The estimated uncertainty in C_f (shown only on the curve for the first trial) is ±0.00036, corresponding to an uncertainty in volumetric flow rate of ±1 sccm. The solid line is a fit to all the points from all three trials using a function of the form:

$$C_f = \alpha_{LV} \mathrm{Re}^n \quad , \tag{9}$$

with fitting parameters $\alpha_{LV} = 0.00164 \pm 0.00006$, $n = 0.61 \pm 0.01$, and a reduced goodness-of-fit parameter $\chi_r^2 = 0.11$.

This Reynolds number dependent flow coefficient, C_f (Re), can be determined for most any component in the manner described above, with the resulting formula for the component's flow coefficient included in the GFSSP user subroutine SORCEF (or, alternatively, BNDUSER).

2.5 Valve Opening

Opening or closing a valve in GFSSP is effected by specifying a variable time-history file for the area of the valve orifice. Under certain conditions, when the valve was opened after some time had elapsed from the beginning of the calculation, it was found that the calculation would show a no-flow condition. In other words, even though the valve was open, no flow would develop, and the pressure downstream of the valve would remain unchanged. This was determined to be the result of the low flow rates that are characteristic of the iSAT PFS; the initial flow rates at the moment a valve opens are very low, so low, in fact, that they fall below the error threshold of the solver. This problem was fixed by momentarily setting the flow rate to a higher value (±0.5 mg/s) at the instant the valve opens. This fix was implemented in the GFSSP user subroutine FLADJUST.

3. SINGLE-PATH MODELING

The iSAT PFS has two propellant lines branching off the single line from the propellant tank: one feeding the HET anode and one feeding the cathode. Flow in each line is controlled by a PFCV. For the purpose of model validation, it is easier to start with a single line as it doesn't have the complication of two interacting branches.

A single-path test line was fabricated at Glenn Research Center (GRC) for cathode testing. Also, a single-path test line was used at Marshall Space Flight Center (MSFC) to study clogging of the propellant lines with redeposited iodine to determine if the formation of a blockage could be detected and could subsequently be cleared. Presented in the rest of this section are the results of simulations of some of the tests performed with these two setups using the GFSSP flow model and compare the computations to experimental data.

3.1 Glenn Research Center Single-Path Test With Iodine

A cathode test was conducted at GRC to evaluate the compatibility of the cathode component materials with iodine and to experiment with the operational parameters required by the cathode design. A schematic diagram of the GRC cathode test line is shown in figure 7 (courtesy of Gabriel Benavides from GRC). The test also provided steady-state single-path iodine flow data that could be compared with the GFSSP flow model. In the test, 305.8 g of iodine were loaded into the propellant tank, and the lines, valves, and pressure sensors were heated until a steady state temperature was achieved. The needle valve and solenoid operated valve (SOV) were then opened and the tank was heated incrementally from 50 °C in 5 °C steps until the desired cathode line pressure was achieved. The test remained at steady state conditions for about 24 hr until the SOV was closed.

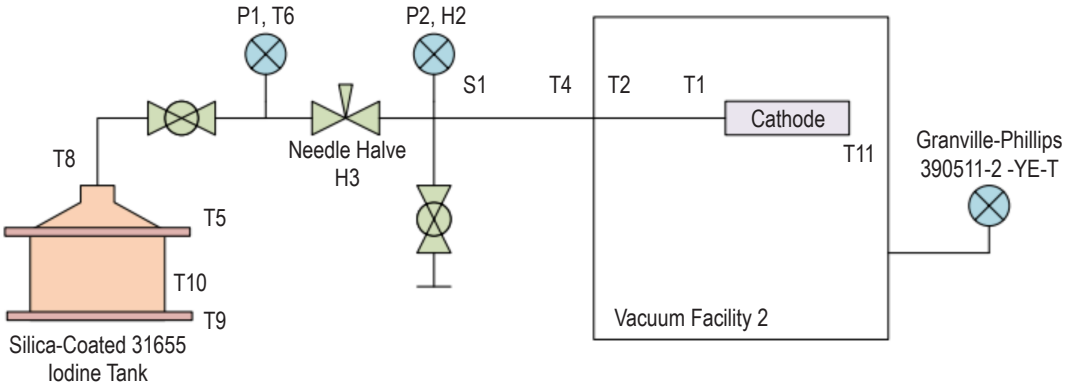

Figure 7. Schematic diagram of the GRC Cathode Test Line.

The corresponding GFSSP flow model is shown in figure 8. The iodine sublimation is modeled as described in section 2.3. The tank ullage volume was estimated using the iodine test mass of 305.8 g and assuming a packing density of 50%. The conjugate heat transfer option in GFSSP was used to model the heating of the ullage by the solid iodine and the 316 SS tank. Since the experimental tank temperature is constant once a steady state pressure is reached, there is an insignificant temperature gradient in the solid and ambient nodes for the model. This effectively insulates the propellant tank and keeps its temperature constant. The model was run at the ultimate steady state pressure of the test, so the computation did not need to be performed for a long period of time to reach equilibrium conditions, having started close to the final conditions.

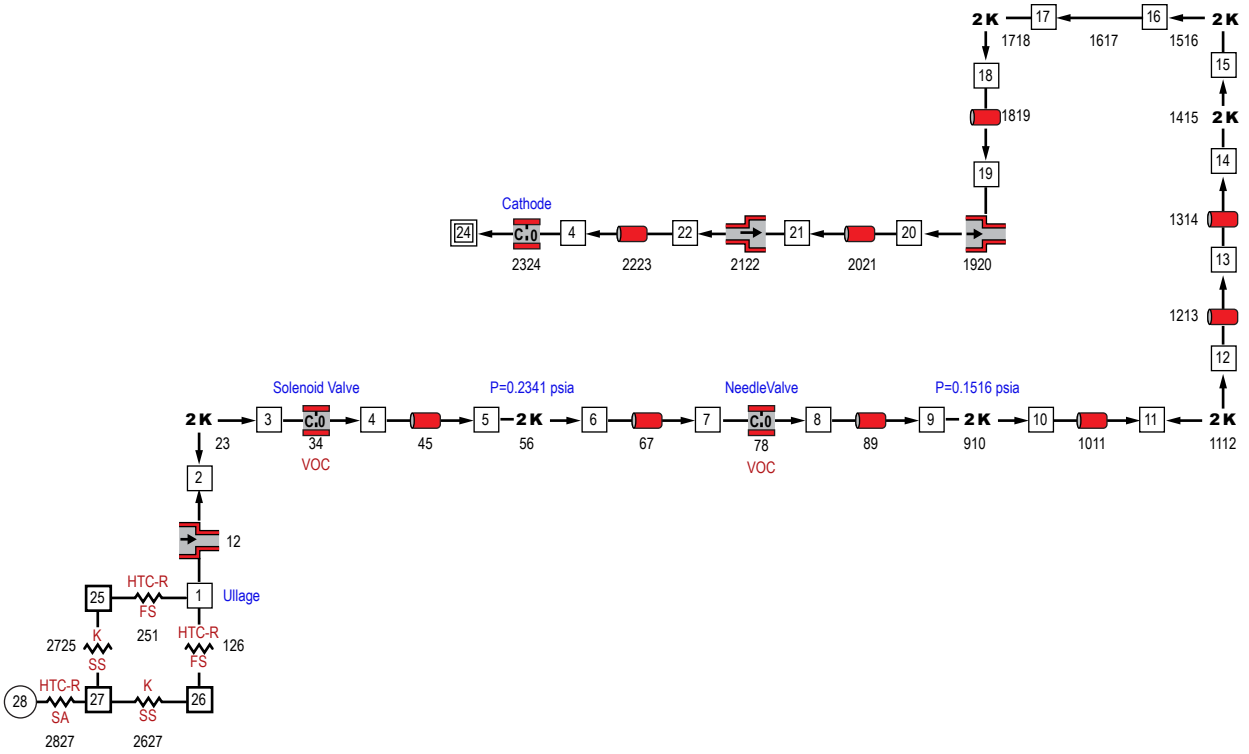

Figure 8. GFSSP model of the GRC Cathode Test Line.

The system is modeled using the wide variety of components that are standard in GFSSP, most of which are well defined. The cathode is modeled as a compressible orifice with a 2×10^{-6} m^2 opening. The two valves are also modeled as compressible orifices; the needle valve and solenoid valve have effective areas of 5.2×10^{-7} m^2 and 2×10^{-5} m^2, respectively.

Data from the GRC test are used to determine the flow coefficients of the valves. The average pressure difference across the needle valve, measured with the two pressure transducers, was used to determine the flow coefficient of the needle valve. A simple GFSSP model with just the needle valve and cathode was used to find an approximate flow coefficient; that value was confirmed with the GRC test model and was determined to be $C_f = 0.1526$. The flow coefficient of the

solenoid valve was determined in a similar manner using the first pressure transducer. It was found that the flow coefficient of the solenoid valve did not significantly change the downstream pressures or flow rates; thus, a standard value of $C_f = 0.6$ was used.

The measured pressures in the tank and the propellant feed line, as well as those calculated with the GFSSP model, are shown in figure 9. The test was run for a little over 20 hr; the calculation was only run out over about 250 s until an approximate equilibrium was reached. The calculated steady state pressure upstream of the needle valve was 1.61 kPa, and that downstream was 1.05 kPa, which differed from the measured values by 4.2% and 6.8%, respectively. For the GRC test, the average flow rate of 2.36 mg/s was determined by measuring the amount of iodine exhausted over 24 hr (203.9 g). The average flow rate calculated with GFSSP was 0.79 mg/s, differing from the measured value by 67%. However, when the GRC test was run a second time with a barium oxide (BaO) emitter, this test lasted 50 hr, and the measured flow rate was 0.78 mg/s.

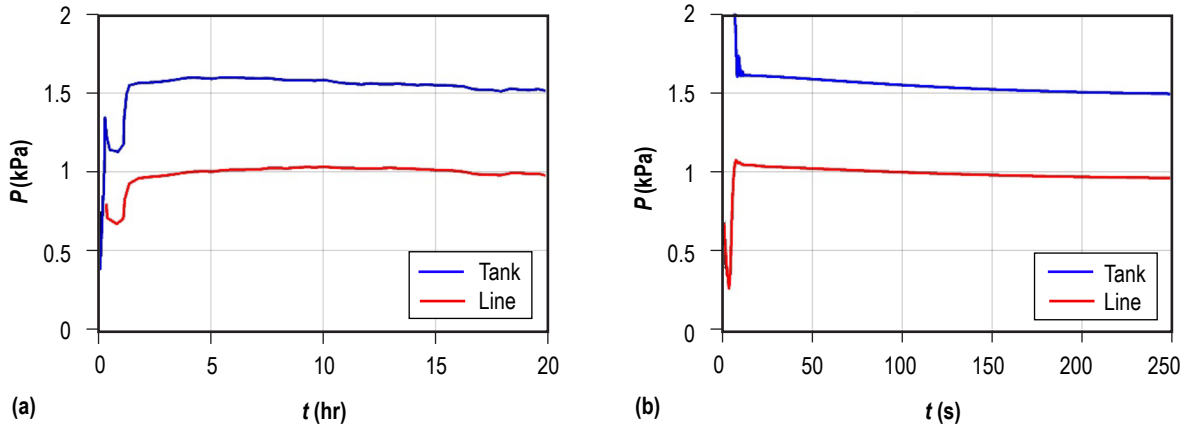

Figure 9. Pressures: (a) measured in the tank and the feed-line from the GRC Cathode Test Line and (b) corresponding and calculated with the GFSSP model.

It should be noted that in the near future GRC will perform cathode line tests with higher accuracy MKSI pressure sensors. The previous test experienced thermal drift and the pressure readings can only be assumed accurate to ≈133 Pa. This is not ideal for correlation with the model.

3.2 Marshall Space Flight Center Single-Path Test With Nitrogen

The GFSSP model of the baseline MSFC single-path test-line, configured for a blow-down test with nitrogen, is shown in figure 10. The test line includes an MKSI 1152C flow controller that, for the purpose of these tests, was used only as a flow meter. A Nupro (Swagelok®, Solon, OH) hand-operated valve (HOV) is located downstream of the flow measurement. Pressures were measured at four stations in the test-line, labeled P1, P2, P3, and P4. The pressure in the vacuum chamber was also recorded throughout the testing. The stations P1 and P2 are the pressure transducers inside the 1152C flow controller. These are MKSI Baratron® gauges that were factory-calibrated

and are temperature regulated. The stations P3 and P4 are strain gauge pressure transducers placed on tees before and after the HOV. The test-line terminates with a 0.71-mm-diameter orifice through which the gas enters the vacuum chamber. It is possible that the effective orifice was actually smaller due to the deposition of iodine from previous tests.

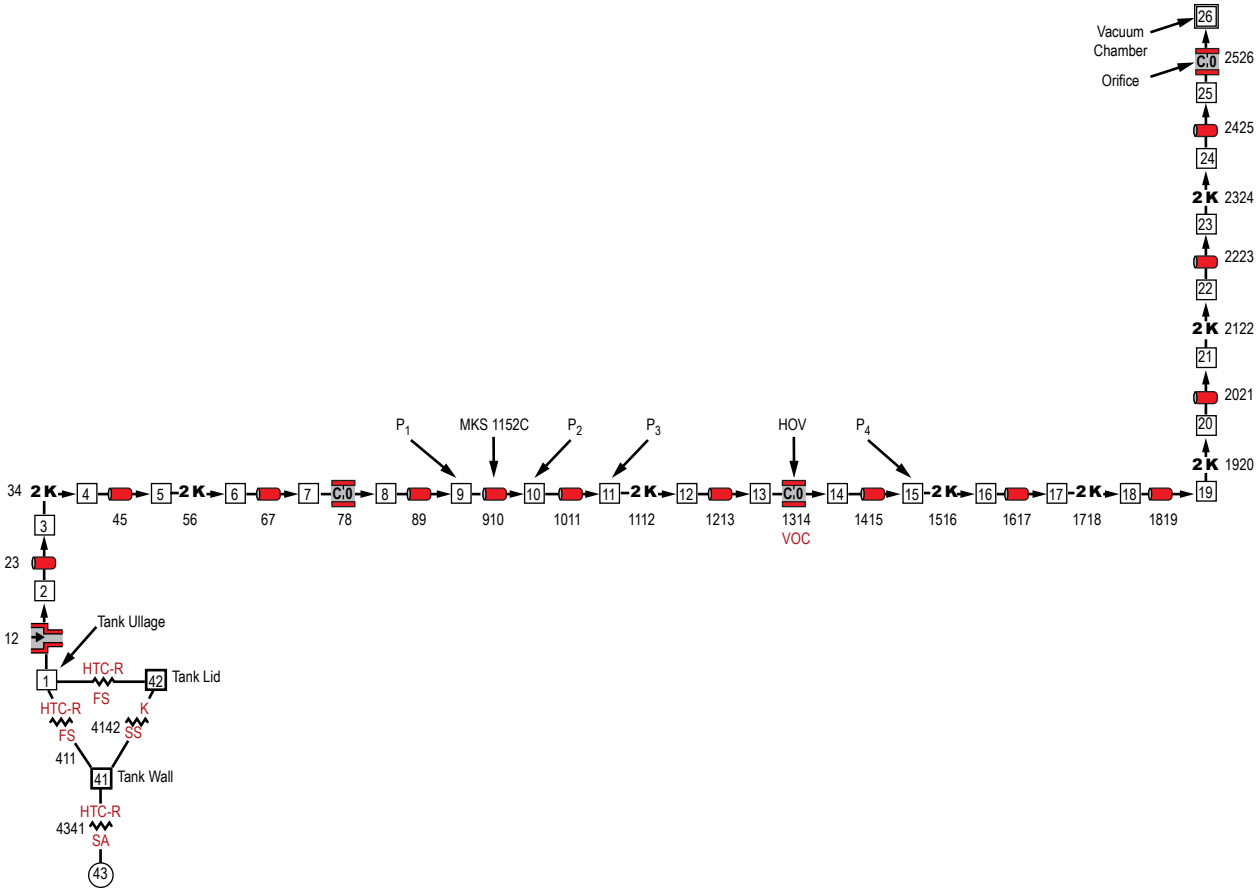

Figure 10. GFSSP model of the MSFC single-path test-line configured for a nitrogen blow-down test. The test-line includes an MKSI 1152C flow controller (here used only as a flow meter) and a Nupro HOV. P1, P2, P3, and P4 indicate stations where pressure is measured.

The flow controller was calibrated for use with iodine; however, it can also be used with nitrogen or any other gas. The mass flow rate was measured using the pressure measurements P1 and P2. They are, respectively, located upstream and downstream of a laminar flow element (LFE) in the 1152C. The LFE consists of a bundle of capillary tubes (M. Townsend, MKSI, private communication, December 2016), and its purpose is to enforce laminar flow in the device so that the mass flow rate may be calculated using the Poiseuille formula:

$$\Gamma = a(P_1^2(t) - P_2^2(t)) \quad , \tag{10}$$

where

Γ = mass flow rate
a = constant, ultimately determined by calibration.

Integrating equation (10) over the interval $t_0 \le t \le t_1$ yields the mass expended from the tank during that time:

$$\Delta m = \int_{t_0}^{t_1} \Gamma(t)dt = a\int_{t_0}^{t_1} (P_1^2(t) - P_2^2(t))dt \quad . \tag{11}$$

The constant a is then given by:

$$a = \left(\frac{\Delta m}{\int_{t_0}^{t_1} \Gamma\left(P_1^2(t) - P_2^2(t)\right)dt} \right) \quad . \tag{12}$$

To use equation (12), the Δm that passes through the flow meter must be calculated or measured independently. In the instance where blow-down data are used to determine this value, a volume upstream of the flow meter is initially pressurized and allowed to flow at time t_0. The value of Δm through the flow meter from time t_0 to time t_1 is determined using the ideal gas law and pressure measurements P1 in upstream volume:

$$\Delta m = \left(\frac{m_m}{k}\right)\left(\frac{V}{T}\right)(P_1(t_0) - P_1(t_1)) \quad , \tag{13}$$

where

m_m = molecular mass of the species (in this case N_2)
V = tank volume plus the line upstream of the valve
T = gas temperature in the tank.

A blow-down test was conducted by charging the tank with N_2 and then opening the HOV to evacuate it to vacuum. The results of the experiment along with that of the corresponding GFSSP calculations are shown in figure 11. For the calculation, the terminal orifice was assumed to have a flow coefficient of $C_f = 0.05$. A variable flow coefficient was specified for the valve (eq. (9)); $C_f = 0.0005 \times \mathrm{Re}^{0.6}$ was found to yield the best overall agreement with the data.

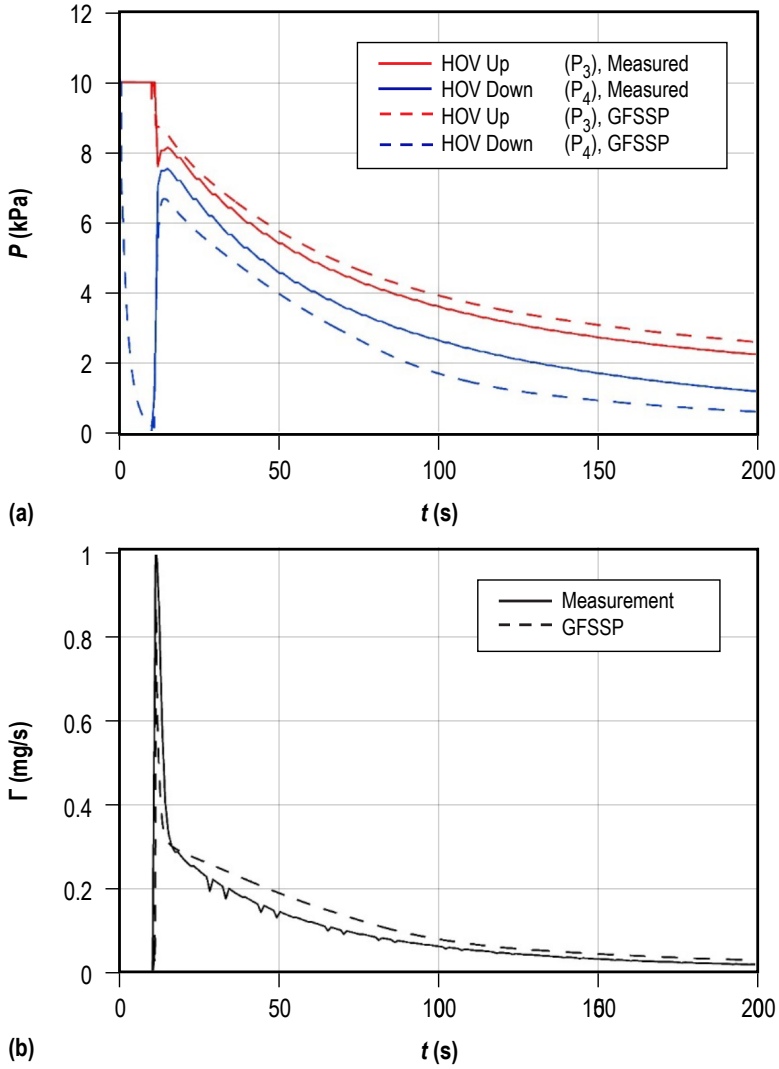

Figure 11. Results of a blow-down test with N_2: (a) pressures upstream and downstream of the HOV, both measured and calculated with GFSSP; (b) measured and calculated mass flow rates.

The GFSSP calculations show qualitative agreement with the data and order of magnitude quantitative agreement. However, attempts to gain better agreement in the calculation by varying the orifice flow coefficient or the effective hydraulic diameter of the LFE did not work and sometimes caused the solutions to become unstable.

3.3 Marshall Space Flight Center Single-Path Test With Iodine

Clogging tests with the MSFC single-path test-line provided an additional opportunity to compare the sublimation model with test data. The GFSSP model used to simulate this test is shown in figure 12. For the first clogging tests, a glass section was added downstream of the HOV so that clogging of the line due to iodine redeposition could be observed. The HOV was left open

and, after the tank had warmed to a temperature of 87 °C, the SOV was opened and the iodine allowed to flow. In the test, the feedline was held at still higher temperature, but heat transfer from this line into the iodine was not modeled. Clogging was observed; however, iodine continued to flow and deposit at the clog site. In that sense, the downstream clog just acted as an iodine sink, having little effect on the source, which continued providing a flow of iodine as if the gas was being exhausted into the vacuum chamber.

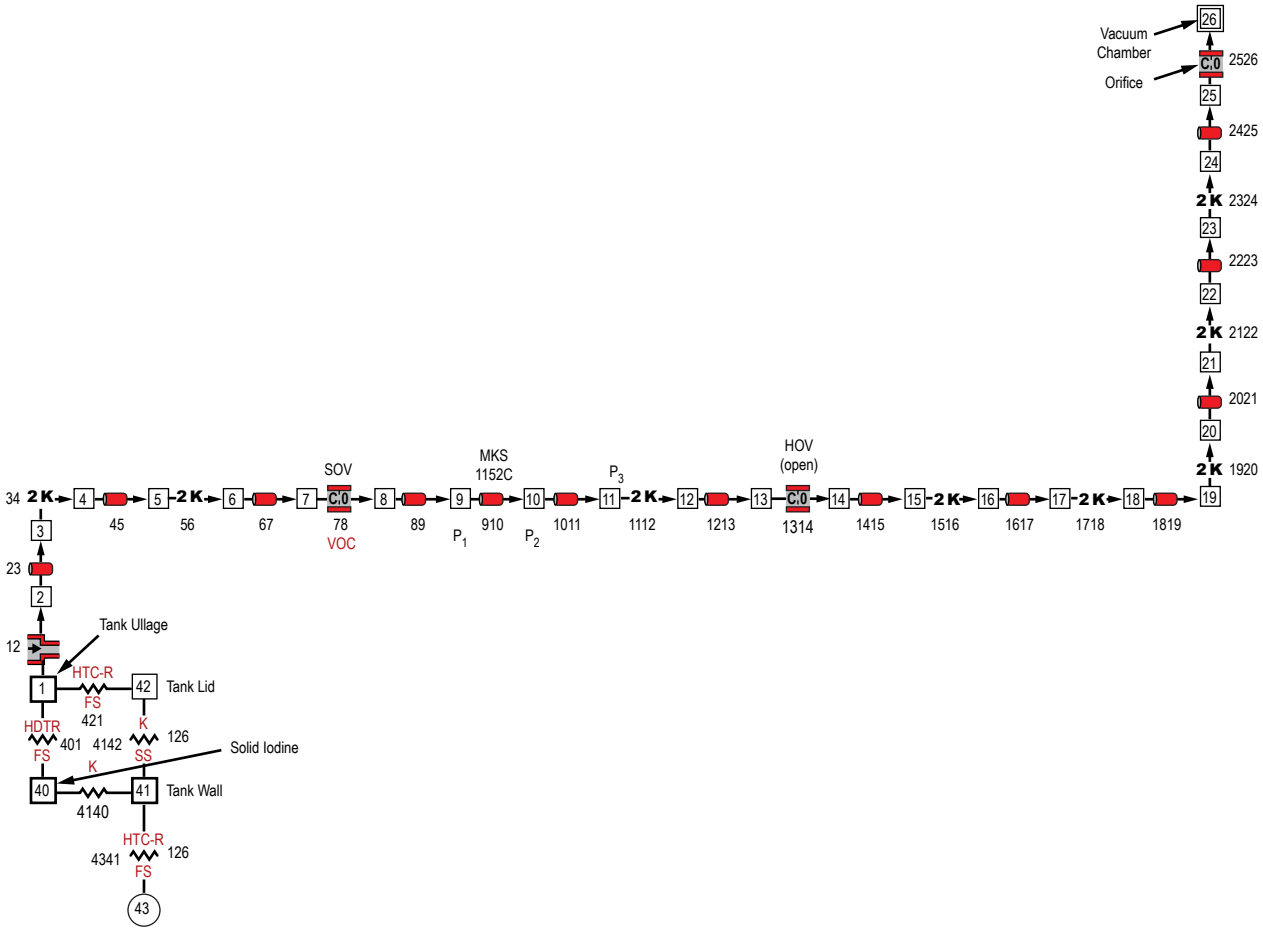

Figure 12. GFSSP model of the single-path test configured for an iodine clogging test. It is the same as that in figure 10, but with the addition of a solid node used to represent the solid iodine. Also, in this case, the HOV is left open, and the SOV is opened from an initially closed state.

The GFSSP model is essentially the same as that used in section 3.2, but with the addition of a solid node representing the solid iodine in the tank. This node is in thermal contact with the tank wall as well as with the vapor in the ullage region. Constant flow coefficients are used throughout. The results of this test, along with the corresponding GFSSP results are shown in figure 13. The initial pressure in the ullage region was chosen to be 4.14 kPa, so as to more closely match the

initial peak in pressure seen in the data; the vapor pressure of I_2 at the initial temperature is 1.52 kPa. The calculated pressures are qualitatively similar to the measured pressures, though the two have significant quantitative differences. The calculated flow rate agrees with the measured flow rate, both qualitatively and quantitatively, and reaches an asymptotic value (i.e., steady state) of about 1 mg/s. In the GFSSP calculation, this asymptotic flow rate was controlled with the choice of the sticking coefficient, α, from equation 8. A number of runs were performed with different values of a until a rough agreement with the measured flow rate was found; the sticking coefficient value that yielded this agreement $\alpha = 1.0 \times 10^{-4}$.

As seen in figures 13a and 13b, the agreement between the measured and calculated pressures is poor, especially the pressure downstream of the flow controller. However, it should be noted that the conditions further downstream of station P2 were less well known (due to the clog that was forming), so it is perhaps unsurprising that the GFSSP model (which assumed an unclogged line) had difficulty in reproducing the pressure. The calculated mass flow rate presented in figure 13c shows relatively good agreement with the measured value, indicating that the GFSSP model is able to simulate the transient sublimation process with a reasonable degree of fidelity.

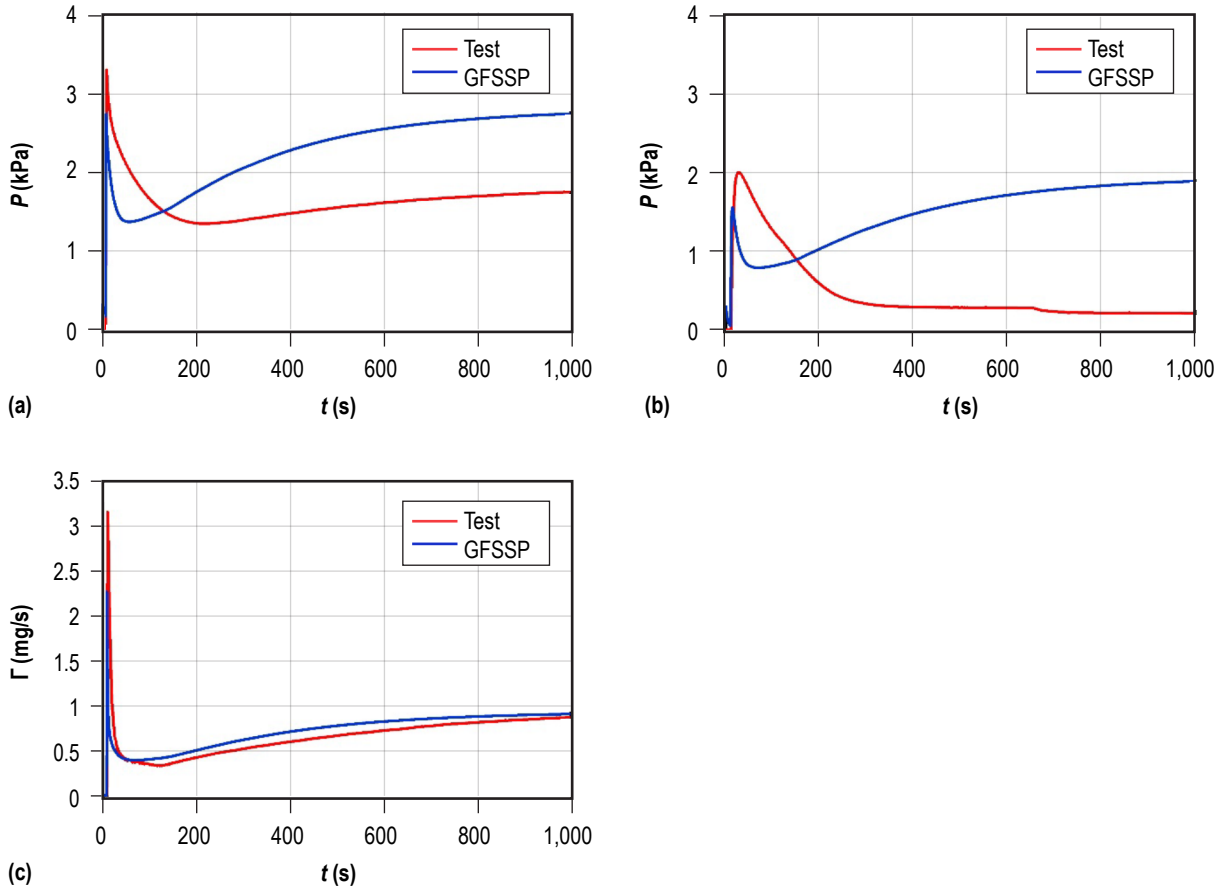

Figure 13. Comparison of test data and the GFSSP model with iodine: (a) pressure at station P1 (from fig. 12), (b) pressure at station P2 (from fig. 12), and (c) the mass flow rate.

4. DUAL-PATH MODELING

The current configuration of the iSAT propellant feed system has two flow paths. Both the thruster and the cathode are fed through lines that branch off from a trunk line connected to the common propellant tank. Each line has its own PFCV to control the propellant flow through it. Modeling of dual-path operation was undertaken to investigate how the two lines might interact, to determine the effects of valve sequencing, and to observe how transients in one line might affect the other.

4.1 Bread-Board Propellant Feed System

A bread-board propellant feed system (schematic shown in fig. 14), based on the current iSAT configuration, was fabricated with the objective of characterizing the behavior of the two PFCVs, which control the propellant flow to the thruster and cathode during flight. This bread-board feed system does not have a thruster or cathode and instead uses metering valves as a stand-in for those devices. The system can be operated with nitrogen, iodine, or any other desired gas.

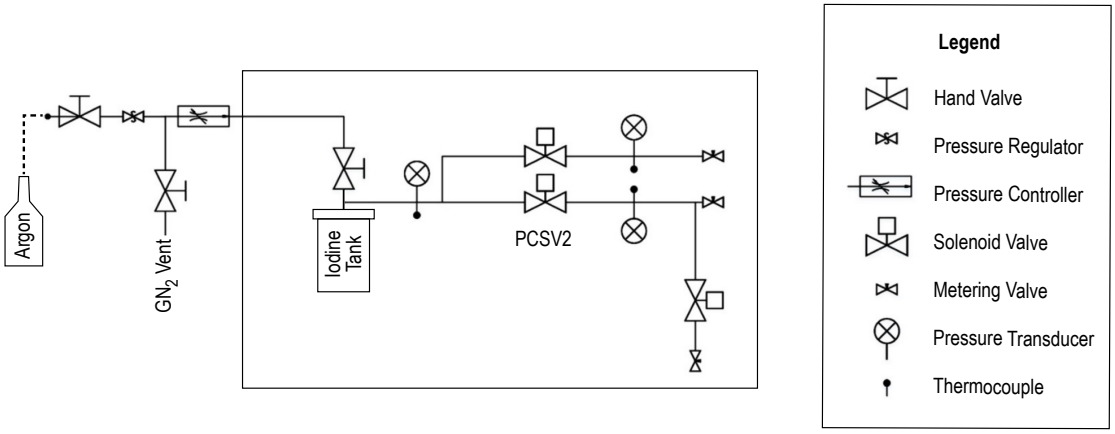

Figure 14. Bread-board propellant feed system for testing the PFCVs and dual flow-path operation.

Although no data are yet available for correlation, the GFSSP model of the bread-board propellant feed system has been developed (see fig. 15) and will be discussed here in further detail. Iodine sublimation is once again modeled as described in section 2.3. The iodine tank used in both the experiment and the model are based on the specifications of the flight tank. The tank ullage volume used in the model is consistent with a propellant mass of 370 g and a packing fraction of 52%. Conjugate heat transfer is implemented to model heating of the ullage vapor by the solid iodine and the Hastelloy® (Haynes International, Inc., Kokomo, IN) C276 tank and lid. Most of

the system components are modeled using standard GFSSP branches. The pressure transducers are modeled with a tee and nodal volumes and will become of importance when data from the test are available.

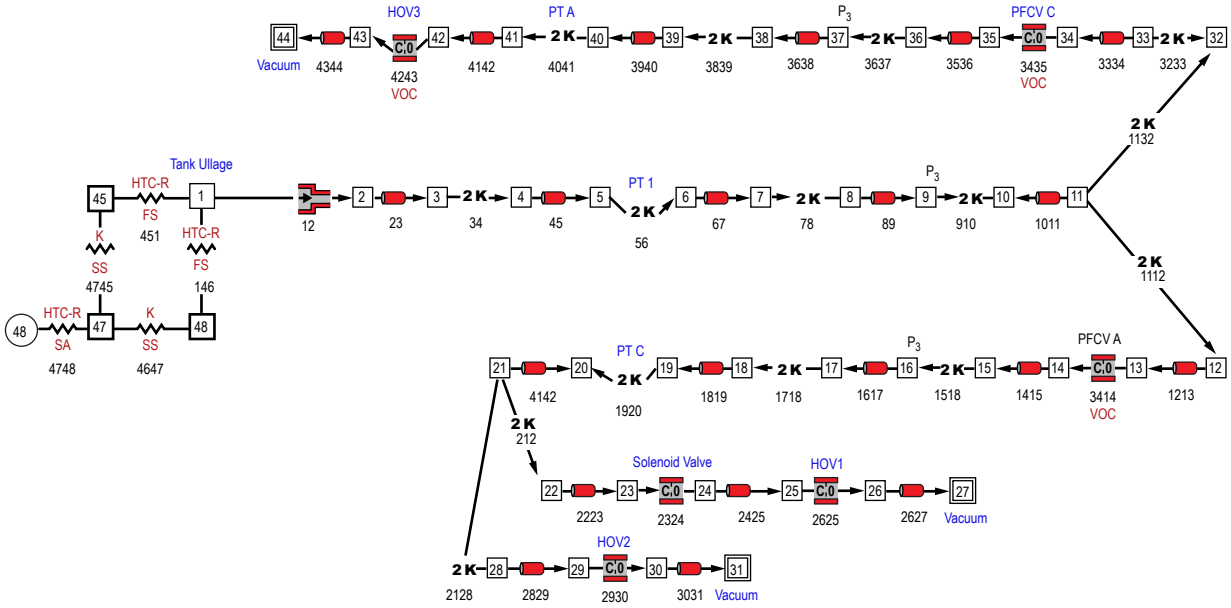

Figure 15. GFSSP model of the dual-path bread-board propellant feed system.

There are several different valves in this experiment: solenoid valves, metering (hand-operated) valves, and the PFCVs. An important outcome of the experiment will be to characterize the flow coefficients of the PFCVs, as they are the only custom components in this feed line test. The other valves are off-the-shelf models, but they are being used outside their nominal operating regimes. Test data will probably be useful in determining the flow coefficients of these components.

In the model, as presently configured, the hand-operated valves and solenoid valves have fixed orifice areas of 1.3×10^{-5} m^2 and 2×10^{-5} m^2, respectively. The PFCVs have an effective orifice area of 8.1×10^{-7} m^2, with inlet and outlet volumes of 1.9×10^{-6} m^3 and 4.6×10^{-7} m^3, respectively. In the present illustrative simulation, the PFCV for the thruster (anode) line opens first at 4.5 s with the cathode PFCV following at 8.5 s. The flow in the cathode PFCV is increased at 4.5 s using the FLADJUST subroutine, as discussed in section 2.5. The initial pressure in the tank is set to the vapor pressure of solid iodine at the temperature of the tank and the solid iodine.

As there are no test data yet, the GFSSP model results, shown in figure 16, can only be considered qualitatively. Figure 16a shows the pressure in the tank (right axis) and the pressures immediately downstream of the PFCVs in both the anode and cathode lines (left axis). Prior to the first valve being opened, the pressure in the tank declines slightly due to redeposition. When the valve is opened at 4.5 s, the pressure in the tank drops sharply as it blows down through the anode line, and the mass flow rate (fig. 16b) spikes up to 7.4 mg/s. When the second valve opens, the tank pressure

drops again. The pressures and flow rate then approach an equilibrium value as sublimated iodine from the tank continuously flows down the feed line. The steady state flow rate out of the tank is 4.3 mg/s, divided evenly between the two lines. In this case, the sticking coefficient used in equation 8 was $\alpha = 2.0 \times 10^{-4}$.

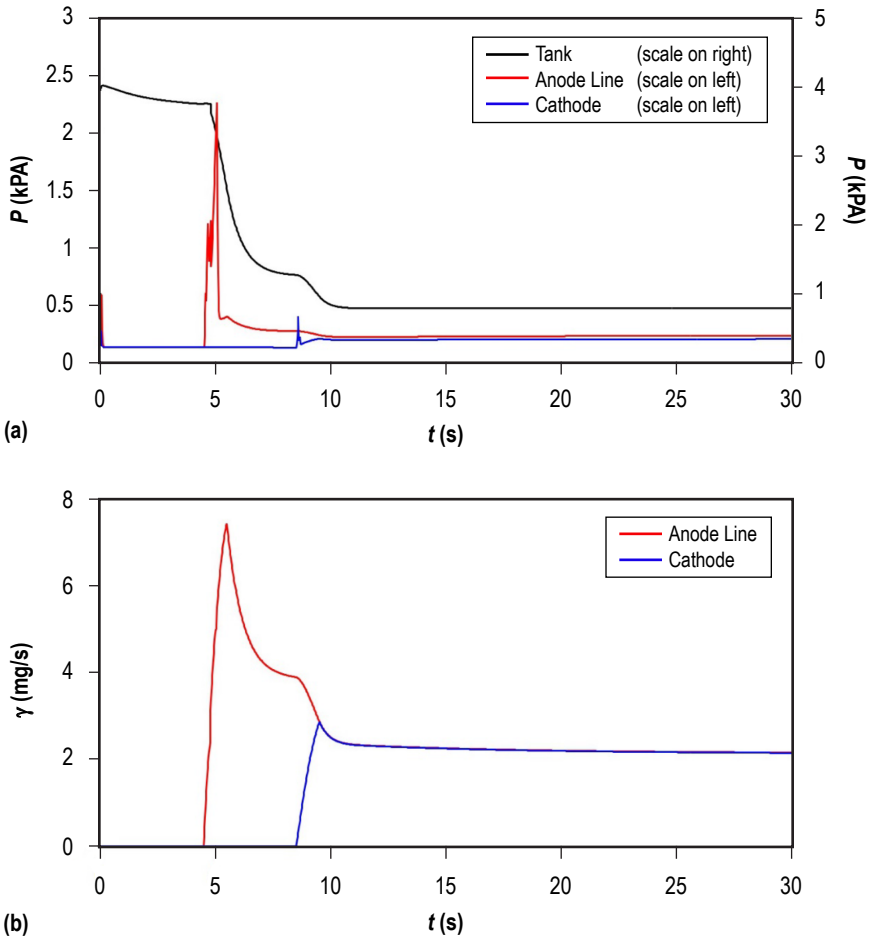

Figure 16. Results of the GFSSP model for the dual-path bread-board propellant feed system: (a) pressures in the tank and immediately downstream of the PFCVs in the anode and cathode lines; (b) mass flow rates in each of the two lines.

4.2 Split-Tank Configuration

Modeling of a split-tank configuration, in which the anode and cathode feed lines are separately fed by two physically-separated halves of a single tank that are in thermal equilibrium, was begun but has yet to yield any useful results. In the model, the two separate lines seem to influence each other, which should not be physically possible. This is perhaps due to the solver employed by GFSSP, which inverts a large matrix to find the solution that globally reduces the error residuals for the entire system. More work will be required for this particular part of the modeling effort.

5. DISCUSSION

With the GFSSP models employed, it has been possible to match qualitative trends observed in actual test data, but achieving quantitative agreement has been more difficult. Most of the feed system can be modeled with standard GFSSP components: pipes, tees, elbows, etc. However, the most critical components—such as the PFCVs, anode, and cathode—are limiting orifices and need to be treated as such. The compressible orifice option in GFSSP has been used for these components. It requires, as inputs, the orifice area and flow coefficient. For the PFCVs, the areas and flow coefficients are not necessarily known at all times.

As was found in testing of the latch valve (described in sec. 2.4), flow coefficients for orifices are expected to be low and highly dependent on the Reynolds number. Typical values for Reynolds number in the iSAT propellant feed system are Re ≤ 100. The mean free path, λ, of an I_2 molecule under the conditions typical for the iSAT feed system can be estimated as:

$$\lambda = \frac{1}{n\sigma} \quad , \tag{14}$$

where

σ = collision cross-section of the molecule
n = number density, given by:

$$n = \rho / m_{I2} \quad , \tag{15}$$

where

$\rho = 0.064$ kg/m^3 (a typical value for iSAT)
m_{I2} = mass of an I_2 molecule (4.23×10^{-25} kg). The cross-section can be estimated as:

$$\sigma = \pi r_{VdW}^2 \quad , \tag{16}$$

where

r_{VdW} = Van der Waal's radius, which for I_2 is 0.198 nm.

Inserting these numbers into equations (14)–(16), the mean free path is $\lambda = 50$ μm. The inner diameter of the tubing used in the feed system is 4.57 mm, about 90 times greater than λ. Boundary layers are typically assumed to be a few hundred mean free paths thick, so one can conclude that the entire iSAT propellant feed system is, under most circumstances, in a highly viscous, boundary-layer-like regime. For the PFCVs, the linear distances could be even smaller, so that not only is the flow highly viscous, but the fluid assumption itself might be violated.

For these reasons, it is perhaps not surprising that it was often difficult to obtain quantitative agreement between the model and test data. The typical flow regimes in iSAT are likely at or beyond the very low end of what GFSSP was developed to simulate.

As a semi-subjective impression, it appeared as though the GFSSP model was better behaved when the fluid used was iodine rather than nitrogen, although the fluid property data for nitrogen is more extensive and of higher quality. This is perhaps just due to iodine being more massive. Mass usually shows up in the denominator of the difference equations for the fluid (as solved), so a higher mass particle would tend to promote numerical stability.

A few blow-down tests with xenon were conducted with the MSFC single-path test setup and simulations were attempted with the GFSSP model. These simulations usually failed in the module that solves the enthalpy equation. It was subsequently found that the default property tables for xenon (which, ultimately, come from NIST), were not defined in a low-enough temperature regime for this problem.

6. FORWARD WORK

As forward work, should it be deemed necessary, the following would be recommended:

- If the GFSSP modeling approach is retained, additional flow testing of the custom components should be performed as described in section 2.4 to characterize them in a detailed fashion. This should be done for the PFCVs and for the anode and the cathode.

- When data from the dual-path flow experiment become available, they should be compared to the output of the model.

- The modeling of a split-tank configuration should be revisited if that option is retained as a possible flight configuration.

- It might be worth considering the development of a dedicated 1D flow modeling code for the iSAT system. In the continuum regime, this could be implemented as a compromise between a full-3D CFD model (which would be impractical) and the lumped-element fluid-circuit approach employed by GFSSP. If the fluid assumption breaks down, the model could potentially solve those areas with a particle solver code.

7. CONCLUSIONS

The modeling of the iSAT propellant feed system using GFSSP has yielded qualitative agreement with test data for blow-down cases with nitrogen and for sublimation-fed cases with iodine. Obtaining quantitative agreement with the data has proved to be more difficult. More data on the behavior of the components in the system would likely help in refining the components in the GFSSP model. However, this does raise the question of the value of such a model in terms of its predictive power if it always requires test data to properly model the system.

REFERENCES

1. Szabo, J.; Pote, B.; Paintal, S.; Robin, M.; Hillier, A.; Branam, R.D.; and Huffman, R.E.: "Performance Evaluation of an Iodine-Vapor Hall Thruster," *J. Prop. Power*, Vol. 28, No. 4, pp. 848–857, 2012.

2. Dankanich, J.W.; Polzin, K.A.; Calvert, D.; and Kamhawi, H.: "The iodine Satellite (iSAT) Hall Thruster Demonstration Mission Concept and Development," Paper Presented at 50th AIAA/ASME/SAE/ASEE Joint Propulsion Conference, Cleveland, OH, July 28–30, 2014.

3. Dankanich, J.W.; Selby, M.W.; Polzin, K.A.; Kamhawi, H; Hickman, T.; and Byrne, L.: "The Iodine Satellite (iSAT) Project Development through Critical Design Review (CDR)," 52nd AIAA/SAE/ASEE Joint Propulsion Conference, Salt Lake City, UT, July 25–27, 2016.

4. Honig, R.E.: "Vapor Pressure Data for the Solid and Liquid Elements," *RCA Rev.*, Vol. 23, pp. 567–586, 1962.

5. Honig, R.E.; and Kramer, D.A.: "Vapor Pressure Data for the Solid and Liquid Elements," *RCA Rev.*, Vol. 30, pp. 285–305, 1969.

6. Majumdar, A.K.; LeClair, A.C.; Moore, R.; and Schallhorn, P.A.: "Generalized Fluid System Simulation Program, Version 6.0," NASA/TP—2016–218218, Marshall Space Flight Center, Huntsville, AL, 884 pp., March 2016.

7. Chase, M.W.: "NIST-JANAF Thermochemical Tables," *J. Phys. Chem. Refer. Data*, Monograph 9, pp. 1417, 1998.

8. Lemmon, E.W.; McLinden, M.O.; and Friend, D.G.: "Thermophysical properties of fluid systems," *NIST Chemistry WebBook*, NIST Standard Reference Database Number 69, P.J. Linstrom and W.G. Mallard (ed.), National Institute of Standards and Technology, Gaithersburg, MD, 2016.

9. Vargaftik, N.B.; and Filippov, L.P.: "Handbook of Thermal Conductivity of Liquids and Gases," *CRC Press,* pg. 36, 1994.

10. Rankine, A.O.: "On the Viscosity of the Vapour of Iodine," *P. Roy. Soc. Lond. A*, Vol. 91, No. 627, pp. 201–208, March 1, 1915.

11. *Eshbach's Handbook of Engineering Fundamentals*, 4th ed., B.D. Tapley and T.R. Poston (eds.) John Wiley and Sons, Inc., New York, pp. 6–11, 1990.

REFERENCES (Continued)

12. Langmuir, I.: "The Constitution and Fundamental Properties of Solids and Liquids: Part I. Solids," *J. Am. Chem. Soc*., Vol. 38, pp. 2221–2295, 1916.

13. Miyamoto, S.: "A Theory on the Rate of Sublimation," *T. Faraday Soc.*, Vol. 29, pp. 794–797, 1933.

REPORT DOCUMENTATION PAGE

Form Approved
OMB No. 0704-0188

1. REPORT DATE *(DD-MM-YYYY)*	2. REPORT TYPE	3. DATES COVERED *(From - To)*
01–10–2018	Technical Memorandum	

4. TITLE AND SUBTITLE

Iodine Propellant Feed System Flow Modeling

5a. CONTRACT NUMBER

5b. GRANT NUMBER

5c. PROGRAM ELEMENT NUMBER

6. AUTHOR(S)

A.K. Martin, P. Sawicki, and K.A. Polzin

5d. PROJECT NUMBER

5e. TASK NUMBER

5f. WORK UNIT NUMBER

7. PERFORMING ORGANIZATION NAME(S) AND ADDRESS(ES)

George C. Marshall Space Flight Center
Huntsville, AL 35812

8. PERFORMING ORGANIZATION REPORT NUMBER

M–1474

9. SPONSORING/MONITORING AGENCY NAME(S) AND ADDRESS(ES)

National Aeronautics and Space Administration
Washington, DC 20546–0001

10. SPONSORING/MONITOR'S ACRONYM(S)

NASA

11. SPONSORING/MONITORING REPORT NUMBER

NASA/TM—2018–220124

12. DISTRIBUTION/AVAILABILITY STATEMENT

Unclassified-Unlimited
Subject Category 20
Availability: NASA STI Information Desk (757–864–9658)

13. SUPPLEMENTARY NOTES

Prepared by the Propulsion Research & Technology Branch, Propulsion Systems Design & Integration Division

14. ABSTRACT

Fluid flow modeling is performed to investigate the behavior of gaseous iodine as a propellant for in-space plasma thrusters. As thermophysical data for iodine are sparse in the operational regime, some properties are derived by extrapolating from existing iodine data, by similarity to available data for other molecules, and through *ab initio* calculations of the thermophysical properties. The modeling exhibits some qualitative agreement, but the viscous nature of the fluid flow and the dependence of the component flow coefficients on the Reynolds number are likely causes of the generally-poor quantitative agreement between the modeling results and experimentally-measured fluid flow properties.

15. SUBJECT TERMS

Iodine, Propellant Feed Systems, Flow Modeling

16. SECURITY CLASSIFICATION OF:			17. LIMITATION OF ABSTRACT	18. NUMBER OF PAGES	19a. NAME OF RESPONSIBLE PERSON
a. REPORT	b. ABSTRACT	c. THIS PAGE			STI Help Desk at email: help@sti.nasa.gov
U	U	U	UU	44	19b. TELEPHONE NUMBER *(Include area code)* STI Help Desk at: 757–864–9658

National Aeronautics and
Space Administration
IS02
George C. Marshall Space Flight Center
Huntsville, Alabama 35812